BeFo

STIFTELSEN BERGTEKNISK FORSKNING
ROCK ENGINEERING RESEARCH FOUNDATION

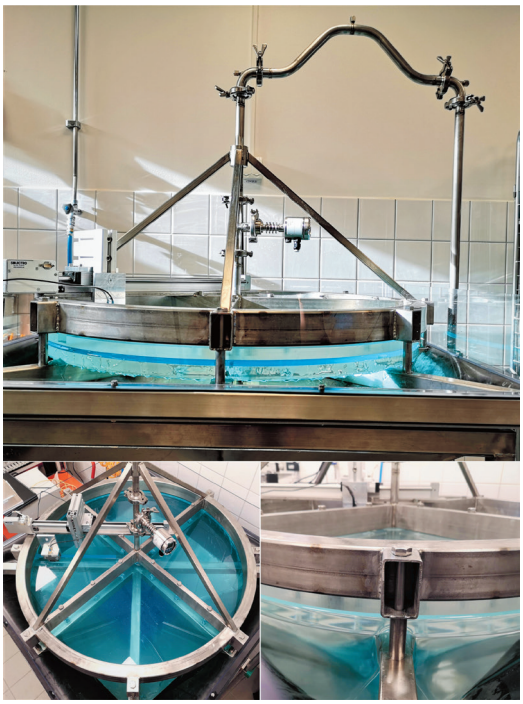

THE BINGHAM-PLUG IN RADIAL FLOW OF A YIELD STRESS FLUID BETWEEN SMOOTH PARALLEL DISKS

John Shamu
Liangchao Zou
Ulf Håkansson

BeFo Report 201

Cover photo: Physical model of the radial flow system.

STIFTELSEN BERGTEKNISK FORSKNING
ROCK ENGINEERING RESEARCH FOUNDATION

THE BINGHAM-PLUG IN RADIAL FLOW OF A YIELD STRESS FLUID BETWEEN SMOOTH PARALLEL DISKS

Including an extended Swedish summary

Binghampluggens utseende vid två-dimensionell radiell strömning

En utökad svensk sammanfattning inkluderas

John Shamu, Royal Institute of Technology (KTH)

Liangchao Zou, Royal Institute of Technology (KTH)

Ulf Håkansson, Skanska Sweden

BeFo Report 201
Stockholm 2020
ISSN 1104-1773
ISRN BEFO-R-201-SE

PREFACE

This work is part of a licentiate assignment at KTH and the BeFo report therefore consists of an English part that is the original Licentiate Kappa (without the journal papers, due to copyright) together with an Extended Swedish Abstract (to cope with the omitted journal papers).

Cement grouting during construction of rock facilities to primarily control water flow in rock fractures is an important, timely and relatively costly operation. By improving prediction, design and grouting operation a better grouting result will be achieved. And in the long run that is the purpose of this research.

This report describes research work performed to further understand the flow of yield stress fluids, flowing radially in planar fractures by using an experimental radial model. This type of flow constitutes the basis for today´s methodology for design of grouting in fractured rock.

At present there exists a controversy, in the grouting community, regarding the prevailing analytical solutions for two-dimensional radial flow of yield stress fluids. The controversy concerns the shape of the plug-flow region at the radial cross-section boundary, where the shear stress is below the yield stress. The question is if the plug is constant, or not, along the penetrated radial distance.

This project aims at verifying the shape of the plug flow region for yield stress fluids in a laboratory model using ultrasound to get a "picture" of the plug region during steady-state flow between Plexiglas plates.

The research presented in this report was mainly carried out at the Division of Soil and Rock Mechanics, at KTH Royal Institute of Technology. Most of the experimental work related to the radial flow model was performed at Incipientus AB, Gothenburg.

The work was carried out by Tafadzwa John Shamu who was supervised by Dr. Ulf Håkansson, Skanska Sweden AB and Dr. Lianchao Zou, KTH, with technical support from Dr. Johan Wiklund at Incipientus AB.
The input from the project reference group is also gratefully acknowledged. The following have participated in the reference group:
Patrik Vidstrand (SKB), Magnus Zetterlund (Norconsult AB), Emmelin Ann (Golder Assoc. AB), Christian Butron (Trafikverket), Liangchao Zou (KTH), Thomas Dalmalm (Trafikverket), Johan Wiklund (Incipientus AB), Mikael Creutz (Golder Assoc. AB), Tommy Ellison (BESAB AB), and Per Tengborg (BeFo).

The project was financed by Rock Engineering Research Foundation – BeFo and Skanska contributed with in-kind support.

Stockholm, 2020

Per Tengborg

FÖRORD

Detta arbete utgör en del av ett licentiat arbete på KTH och består av den engelska original Kappan (utan artiklar pga copyright) samt en utökad sammanfattning på svenska (för att kompensera för de utlämnade artiklarna).

Cementinjektering i samband med bergbyggnad för att i första hand kontrollera vattenstömning i bergssprickor är en viktigt och en tidkrävande och förhållandevis kostsam operation. Genom att förbättra prognostisering, design och utförande av injektering kan man få ett bättre slutresultat. Det är i förlängningen vad denna forskning syftar till.

Föreliggande rapport beskriver forskning som utförts för att ytterligare förstå radiell strömning av vätskor med flytgräns i plana sprickor med hjälp av en laboratoriemodell. Denna typ av strömning utgör basen i dagens metodik för uppskattning och projektering av injektering i sprickigt berg.

Inom dagens injekteringsforskning råder det delade meningar beträffande de analystiska lösningar som finns för två-dimensionell radiell strömning för vätskor med flytgräns. Meningsskiljaktigheterna handlar om Bingham-pluggens utseende i det område av flödet där skjuvspänningen är lägre än flytgränsen. Frågeställningen är om pluggen är konstant, eller inte, utmed vätskans inträngningslängd vid en given tidpunkt.

Detta projekt har som målsättning att verifiera pluggens utseende för vätskor med flytgräns, i laboratoriemiljö med hjälp av ultraljud, vid stationärt två-dimensionellt flöde mellan två cirkulära plexiglasskivor.

Forskningen som presenteras i denna rapport har främst utförts på Avdelningen för Jord- och Bergmekanik på KTH och det experimentella arbetet har gjorts hos Incipientus AB, Göteborg.

Arbetet har utförts av Tafadzwa John Shamu och handletts av Dr. Ulf Håkansson, Skanska Sverige AB och Dr. Liangchao Zou, KTH, med teknisk assistans från Dr. Johan Wiklund, Incipientus AB.

Projektets referensgrupp har bistått projektet med råd och bestod av Patrik Vidstrand (SKB), Magnus Zetterlund (Norconsult AB), Emmelin Ann (Golder Assoc. AB), Christian Butron (Trafikverket), Liangchao Zou (KTH), Thomas Dalmalm (Trafikverket), Johan Wiklund (Incipientus AB), Mikael Creutz (Golder Assoc. AB), Tommy Ellison (BESAB AB) och Per Tengborg (BeFo).

Projektet finansierades av Stiftelsen Bergteknisk Forskning – BeFo och Skanska bidrog med stöd genom in-kind.

Stockholm, 2020

Per Tengborg

SUMMARY

The rheological properties of cement-based grouts play a key role in determining the final spread in grouted rock formations. Rheologically, cement grouts are known to be complex thixotropic fluids, but their steady flow behavior is often described by fitting the simple Bingham constitutive law to flow curve data. The Bingham model is a rheological flow model that simplifies the description of the flow of yield stress fluids (YSFs) such as cement-based grouts. The resultant Bingham parameters are then used in grouting design of e.g. tunnels, to estimate the penetration length.

As part of the licentiate work carried out at KTH, the work presented in this report focuses on the measurement of velocity profiles of a model yield stress fluid (Carbopol) within the radial flow geometry. Radial flow between parallel plates, is an idealized fundamental flow configuration that is often used as a basis for grout spread estimation in planar rock fractures. Compared to other flow configurations with YSFs, e.g. channels, only a limited amount of work has presented analytical solutions, numerical models and especially experimental work for radial flow. Thus, as a first step towards more systematic studies of the plug flow region of YSFs in radial flow the current work presents the design, manufacture and for the first time velocity profile measurements that were conducted by using the pulsed Ultrasound Velocity Profiling (UVP) technique. The current observations for tests carried out with different disk spacings and flow rates show a distinct plug region, coupled with wall slip effects for the Carbopol model YSF fluid that was used. The theoretically predicted velocity profiles and the measured ones agree reasonably well, and the main discrepancies are discussed. Future studies would then be targeted at improving the current experimental setup, for detailed measurements of the plug flow region along the radial length, which remains a challenging issue for studies on YSFs and engineering applications such as rock grouting design.

Keywords

Cement-based grouts, grouting, yield stress fluid (YSF), thixotropy, critical shear rate, radial flow, wall slip, Bingham model

SAMMANFATTNING

Cementbaserade injekteringsmedels reologiska egenskaper har en stor påverkan på strömning och inträngningslängd i sprickigt berg. Medlens reologi är komplex, inklusive tixotropi, men strömningen beskrivs ändå oftast med den enkla linjära Bingham modellen i injekteringssammanhang. De två parametrarna från denna modell, flytgräns och viskositet, används sedan inom injekteringsdesign, för t.ex. tunnlar och dammar, för att bedöma inträngningen.
Ett annat fokus i licentiatarbetet har varit att studera icke-Newtonska modellvätskors (Carbopol) radiella strömning mellan parallella plattor. Denna typ av strömningsgeometri används ofta som en idealiserad konfiguration för strömning i bergsprickor. I jämförelse med andra enklare geometrier, finns endast en begränsad forskning utförd för denna geometri både då det gäller analytiska och numeriska beräkningar men framförallt då det gäller experiment. Som ett första steg inför en mer systematisk undersökning av icke-Newtonsk radiella strömning presenteras i detta arbete framtagandet av en fysisk laboratoriemodell där hastighetsprofilerna mellan plattorna för första gången visualiserats med hjälp av ultraljud. De utförda mätningarna med tre olika öppningar mellan plattorna sam tre olika värden på det konstanta flödet, visar på en distinkt plugg som är ett resultat av vätskans flytgräns samt glidning i gränsskiktet mellan vätskan och plattornas fasta begränsningsytor. En jämförelse mellan uppmätta hastighetsprofiler och analytiskt beräknade diskuteras där resultaten överensstämmer relativt väl, med beaktande av de långtgående förenklade antaganden som krävs för beräkningarna.
Fortsatta studier kommer att fokuseras på att förbättra laboratoriemodellen för en mer detaljerad studie av icke-Newtonska vätskors strömning och hur pluggen utvecklas under den radiella inträngningen, vilket fortsättningsvis är av betydelse för design av injektering i bergsprickor.

Nyckelord: Cementbaserade injekteringsmedels, plugg, Bingham modellen, tixotropi, radiella strömning, glidning

MAIN REFERENCED DOCUMENTS

The work presented in this report makes reference to a submitted scientific journal paper and the original licentiate thesis:

Shamu, Tafadzwa John, Liangchao Zou, R Kotzé, Johan Wiklund, and Ulf Håkansson. "Radial Flow Velocity Profiles of a Yield Stress Fluid between Smooth Parallel Disks." Submitted to Rheologica Acta, April 2019.

J. Shamu, "On the measurement and application of cement grout rheological properties," Licentiate thesis Stockholm: KTH Royal Institute of Technology, TRITA-ABE-DLT, 1922, 2019.

Contents

1. INTRODUCTION

1.1 Background

Cement-based grouting of rock fractures to minimize water inflows into underground constructions e.g. in tunnels is common practice, especially in Scandinavia (Hässler, 1991; Håkansson, 1993; Stille, 2001; Funehag, 2007; Gustafson et al., 2013; Fransson et al., 2016; Nejad Ghafar, 2017; Rahman et al., 2017; Zou et al., 2018; Zou et al., 2019).

The widespread use of cement-based grouts is due to their relatively low cost, combined with the fact that they pose less of a risk as a pollutant especially to underground water resources when compared to other chemical-based grouts. The effectiveness of the grouting process depends on several factors, with the main ones being: rock fracture geometry, grouting design and execution, as well as the penetrability and rheological flow properties of the cement grouts that are used. It has been shown analytically and through experiments, that the rheological properties of cement grouts significantly influence grout propagation during the grouting process, and consequently the final spread and sealing effect that can be achieved in grouted rock fractures (Håkansson, 1993; Gustafson et al., 2013).

In relation to cement grout flow in rock fractures is the principle of radial flow of Bingham type fluids between smooth parallel plates. Radial flow in which a fluid penetrates the center of two disks and flows out radially is of interest to applications such as rock grouting design. This fundamental flow configuration ideally simulates cement grout propagation from a central injection borehole from where the grouts spread radially outward into surrounding fractures. The *plug-flow region*[1] of the velocity profile of a YSF is directly related to the yield stress property of the fluid, since the plug region is an unsheared region, wherein the shear rates are close to zero and shear stresses are below the yield stress. Only a limited amount of works have presented analytical and numerical solutions describing the expected velocity profiles for YSFs in this flow geometry. Thus, an experimental study as a first step towards verifying existing theory, together with the measurement of the shape of the plug flow region across the radial length also formed a major part this work.

1.2 Project aims

The aims of the project work were as follows:

(i) To design an experimental radial flow model that is to be used for studying radial flow velocity profiles of a model YSF (Carbopol).

(ii) The model is to be equipped with instrumentation, consisting of an acoustically characterized ultrasound sensor, which is an integral part of the (Ultrasound Velocity Profiling) UVP system to be used for velocimetry.

[1] The ***plug-flow region*** is the central region in the velocity profile of a yield stress fluid that flows within a confined flow geometry e.g. radial flow. Within the plug-flow region, the fluid is not sheared and moves as a 'solid-like' plug since the shear stresses within this plug-flow region are below the yield stress of the fluid. For a particular flow geometry, the extent/size of the plug-flow region is related to the yield stress value of the fluid. In this work we have used the Herschel Bulkley (HB) rheological model instead of the common Bingham model to describe the rheological properties and analytical solutions to radial flow since the HB-model better describes yield stress fluid flow particularly at very low shear rates. Other terms synonymous to the plug-flow region used in this report and in literature are: unsheared region, Bingham plug, the plug, plug.

(iii) Develop a preparation procedure for Carbopol fluid that can be used for velocimetry whilst maintaining the desired simple YSF behavior (non-thixotropic).

(iv) Lastly, the objective is to measure for the first time, time-averaged velocity profiles within the radial flow geometry. The ultimate goal in subsequent studies is to use the developed model to study in detail the nature of the plug flow region.

1.3 Limitations of the current work

The limitations of the current work are mainly based on the measurement techniques that were used, i.e. Pulsed Ultrasound Velocity Profiling (UVP). With UVP, the spatial and lateral resolution could have been improved by using a higher frequency transducer. Also some limitations due to the bending of plexiglass disks were encountered; these led to reduced accuracy especially in flow rates comparisons between measured data and the analytical solutions. These limitations were then taken into account as suggestions for future work.

2. THEORY AND LITERATURE REVIEW

Section 2.1 mainly describes the relevance of the radial flow configuration to grouting applications by describing some of previous work that has been carried out thus far.

2.1 Velocity profile measurements of a YSF in radial flow

2.1.1 Radial flow: relevance to grouting applications

When grouting design is carried out several assumptions and simplifications are carried out in order to estimate the propagation and spread of grouts in fractures (Hässler, 1991; Håkansson, 1993; Stille, 2015; Zou et al., 2018). Cement grout rheological behavior is often simplified by using constitutive laws e.g. the Bingham model. When combined with the rock fracture geometries the entire flow configurations can then be approximated as one-dimensional (1D) channel flow and two-dimensional (2D) flow e.g. radial flow between parallel disks. An illustration of such simplifications is depicted in Figure 2.1.

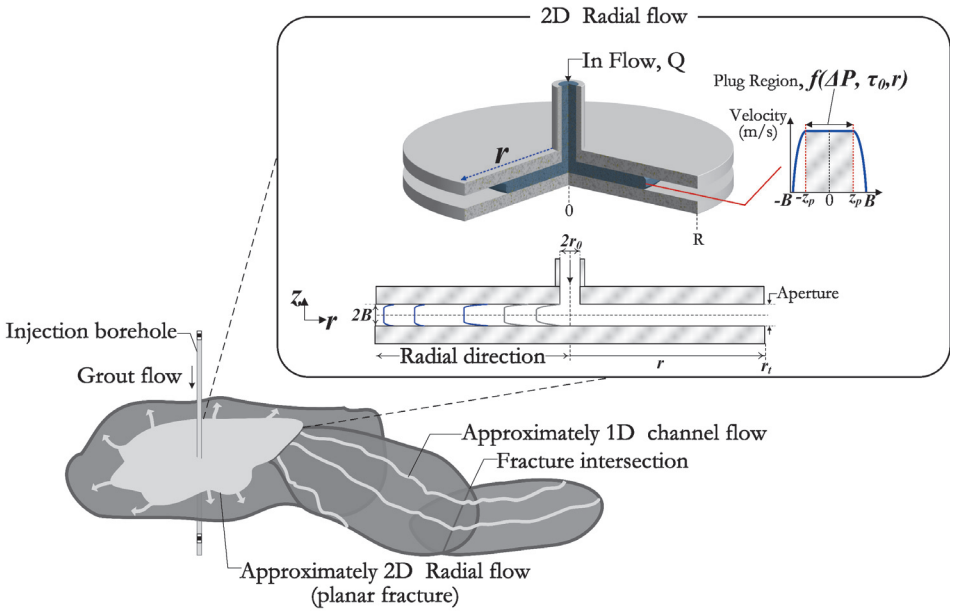

Figure 2.1. Schematic illustrating the idealized 1D channel and 2D radial flow between parallel disks, adapted from (Zou et al., 2018).

A number of analytical solutions describing the flow of Bingham fluids between parallel disks have been presented in the literature (Dai & Byron Bird, 1981; Lipscomb & Denn, 1984; Huang et al., 1987; Gustafson & Stille, 2005; El Tani, 2012; Gustafson et al., 2013; El Tani & Stille, 2017). Usually the underlying assumptions that are used to derive these analytical solutions are that: the aperture is constant throughout the radial length, cement grouts as Bingham fluids are incompressible, the flow is laminar and developed, and that the lubrication approximation (i.e. the aperture dimension is much smaller than the radial length)

is valid. Although these analytical models facilitate the estimation of grout penetration, it has to be mentioned that they are largely simplifications especially when the actual geometry of fissures is unknown and the validity of such approaches still needs to be verified for different apertures and fluids (Frigaard et al., 2017).

For this work a constant flow rate analytical solution for yield-power-law (HB) fluids is presented for verification of the measured velocity profiles. The solution is described here as outlined in the referenced in (Zou et al., n.d.).

Based on the assumption of lubrication approximation, the analytical velocity profiles for incompressible yield-power-law fluids, steady-state, laminar, radial flow between parallel disks can be expressed as

$$v_z^f(z_p < z \leq B) = \frac{n}{n+1}\left(-\frac{1}{k}\frac{\partial P}{\partial r}\right)^{\frac{1}{n}}\left[\left(B - z_p\right)^{\frac{n+1}{n}} - \left(z - z_p\right)^{\frac{n+1}{n}}\right] \tag{1}$$

$$v_z^p(0 \leq z < z_p) = \frac{n}{n+1}\left(-\frac{1}{k}\frac{\partial P}{\partial r}\right)^{\frac{1}{n}}\left(B - z_p\right)^{\frac{n+1}{n}} \tag{2}$$

where v_z^f is the velocity for the yielding flow parts between the edges of plug flow region (z_p) and the walls (B), v_z^p is the velocity for the plug flow region, $\frac{\partial P}{\partial r}$ is the pressure gradient, r and z are the radial and vertical coordinates, k is the consistency coefficient, n is the flow index, and z_p is half of the plug flow region (Figure 2.1), expressed as

$$z_p = \frac{\tau_0(r_t - r_0)}{(P_1 - P_2)} \tag{3}$$

where τ_0 is the yield stress, P_1 and P_2 are the pressure at the inlet r_0 and outlet r_t. The flowrate Q is obtained by integration of the velocity over the aperture, written as,

$$Q = \int_0^B 4\pi r\, v_z\, dz = \frac{4\pi r n}{n+1}\left(-\frac{1}{k}\frac{\partial P}{\partial r}\right)^{\frac{1}{n}} B^{\frac{2n+1}{n}}\left(1 - \frac{z_p}{B}\right)^{\frac{n+1}{n}}\left[1 - \frac{n}{2n+1}\left(1 - \frac{z_p}{B}\right)\right] \tag{4}$$

2.1.2 A review of radial flow experiments of yield stress fluids

For the purposes of validating analytical predictions, experimental studies are carried out to verify the extent to which theoretical assumptions are valid and how they can be further developed based on experimental observations. For instance in the case of 1D YSF flows in, e.g. channels and pipes, several studies and papers have reported analytical solutions, together with experimental investigations and numerical simulations extensively describing these flow configurations (Chhabra & Richardson, 2008). With the use of velocimetry and flow visualization methods such as Particle Image Velocimetry (PIV), Magnetic Resonance Imaging (MRI) and pulsed Ultrasound Velocity Profiling (UVP), experimental studies validating theory have shown in detail, the shape of laminar flow velocity profiles for different YSFs within these flow configurations (McCarthy et al., 1997; Pfund et al., 2006; Birkhofer, 2007; Powell, 2008; Wiklund et al., 2007; Kotze et al., 2012; Rahman et al., 2017).

In contrast, only a limited number of experiments on 2D radial flow of YSFs has been carried out.

Some of the earliest experimental work conducted by e.g. Laurencena & Williams (1974), compared radial flow measurements of the pressure distribution along the radial length, as well as the measured flow rates to analytical predictions, whilst using different power-law fluids, including Carbopol gels, which are also used in our current study. The results from their work showed a good agreement between theoretical predictions and the measurements; however, they strongly suggested that elasticity-induced secondary flows and flow instabilities are highly expected for more concentrated polymer gels as evidenced with tracer injections in their experiments. More recently, the work by Majidi et al. (2010) also presented flow rates and pressure distributions with Xanthan gum as the test fluid. The numerical and measured data satisfactorily agreed with the analytical solutions based on the yield-power-law fluid model. The main discrepancies in their data at high flow rates were explained by the enlargement of the aperture due to pressure build up. Most of the radial flow experiments that have been carried out in relation to grouting have mainly focused on determining the validity of analytical predictions for grout penetration length, whilst using the Bingham model for cement grouts (Funehag & Thörn, 2018; Mohammed, 2015).

Thus, the work presented in this report was aimed at (apparently for the first time), measuring radial flow velocity profiles of a model YSF, to further investigate the nature of these profiles and the shape of the plug flow region, within the current framework grouting research.

3. EXPERIMENTAL METHODS AND PROCEDURES

3.1 Radial flow experiments

Firstly, a description of the radial flow model design is presented under Section 3.1.1. Secondly, the Ultrasound Velocity Profiling (UVP) method and acoustic tests, to define the critical Doppler angle and sound velocity that are required for velocimetry are presented. Lastly, the preparation of the model YSF Carbopol is then presented together with the rheological flow curve test.

3.1.1 Radial model design

The initial design of the physical radial model was based on earlier models presented in the literature (Savage, 1964; Laurencena & Williams, 1974). The aim was to have a radial flow area that was clear of intrusive objects e.g. fasteners, in order to clearly study the underlying radial flow of Carbopol. The entire setup including an image of the actual model used is shown in Figure 3.1.

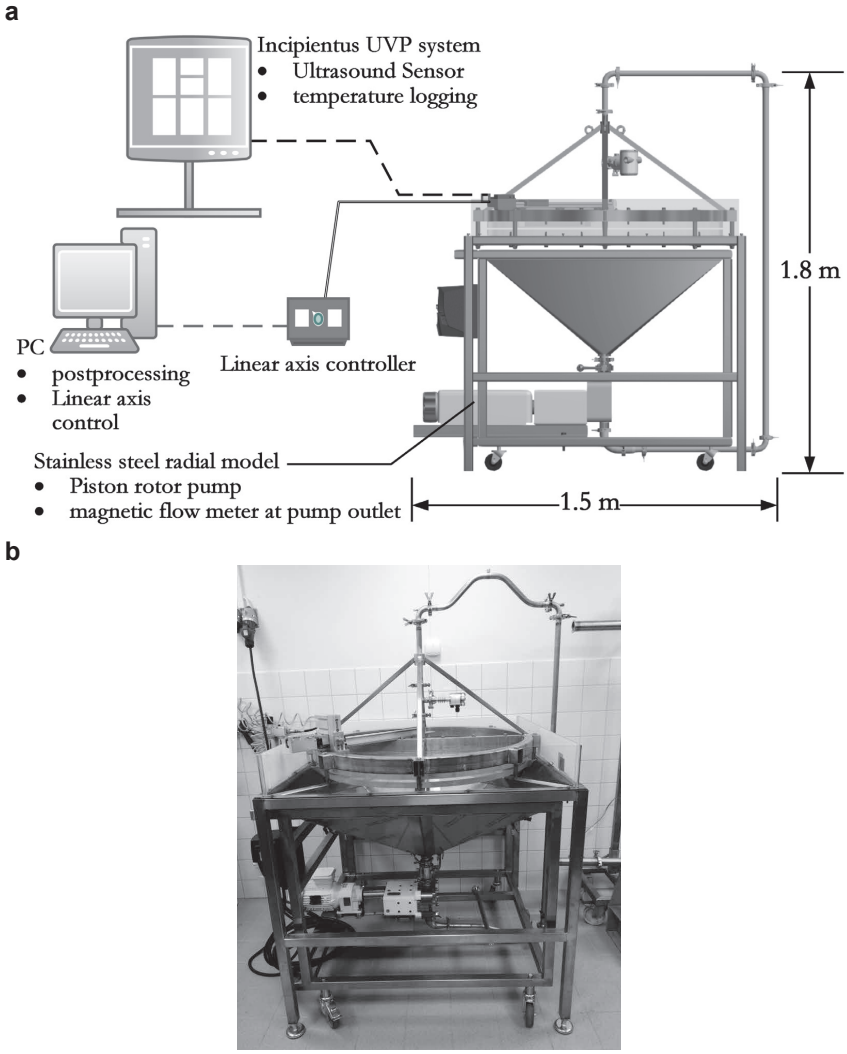

Figure 3.1. (a) A schematic of the radial flow system (b) An image of the physical model

The system components included a magnetic flow meter (Discomag DMI 6531, Endress + Hausser) at the pump outlet and a PT100 temperature transducer. A piston rotor pump was used to pump the fluid at set flow rates controlled from a variable speed drive (VSD). The fluid then circulated from the bottom of the tank into the radial flow area where measurement was carried out. A motorized linear axis (Isel LEZ 1) with a repeatability of ±0.2 mm was then used to move the ultrasound sensor (US) used for velocimetry, to different radial locations. Schematics and images of the linear axis-slot setup and the radial model are shown in Figure 3.2.

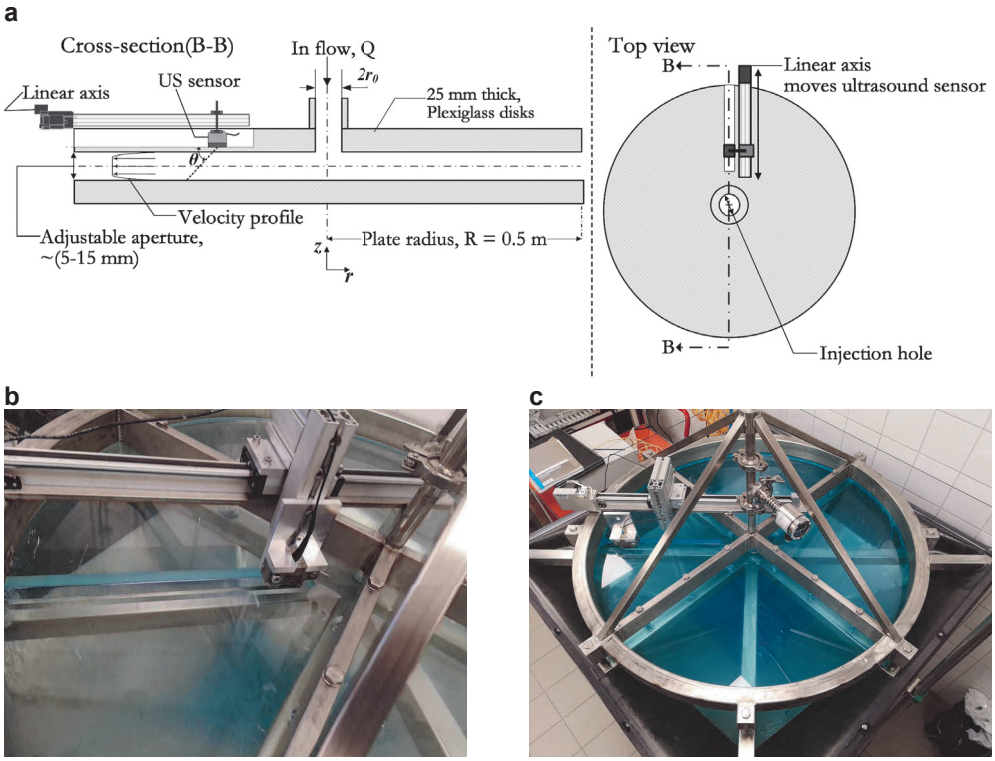

Figure 3.2. (a) schematic of the linear axis setup (b) image showing ultrasound sensor in slot (c) top view image of spoke frame and radial model

The slot shown in Figure 3.2b was machined on the top disk to allow sufficient propagation of the ultrasound beam, without significant attenuation. After machining the wall thickness in the slot was 5 mm. The desired gap (aperture) was achieve by a metallic spacer system around the periphery of the disks. The top spoke frame was used as a support for the top disk, aimed at maintaining the set aperture even during high flow and pressure conditions. The uplift expected during flow conditions was also simulated in the design stage by using a Computer Aided Design (CAD) model developed within Autodesk Inventor® simulation package. From this test, the thickness of the frame members to be used were adjusted such that only negligible uplift (~0.25% displacement in vertical direction) was noted; thus, all tests were considered to be conducted under constant aperture conditions.

3.1.2 Ultrasound Velocity Profiling (UVP) and Acoustic tests

The UVP method used to measure velocity profiles, is a velocimetry method that has been used to acquire velocity profiles in a wide range of complex fluids (Satomura, 1957; Takeda, 1991; Dogan et al., 2005; Pfund et al., 2006; Wiklund et al., 2007; Birkhofer, 2011; Kotze et al., 2012; Takeda, 2012; Rahman et al., 2017). The method relies on the detection of frequency shifts between successive reflected pulses when preprogrammed ultrasound pulses are transmitted into the medium under study. Depending on the flow configuration pulses received from different depths are processed using signal processing algorithms,

transforming the measured doppler frequencies (frequency shifts) into velocities that constitute the velocity profile (Barber et al., 1985; Jensen, 1996; Ricci & Meacci, 2018).

The individual velocities v_i at each point of the flow geometry where the velocimetry is carried out are calculated as,

$$v_i = cf_{d_i}/2f_0 cos\theta \tag{8}$$

where f_0 is the central ultrasound transmission frequency, c is the velocity of sound, f_{d_i} the Doppler shift frequency for particles flowing at a certain distance position (gate) and θ is the Doppler angle.

Several studies have shown that the accuracy of velocity estimation depends on the correct determination of the sound velocity in the fluid under study as well as the Doppler angle θ. The error contribution from incorrect angle values is quite significant, therefore, in this work the measurement of this angle was carried out in detail using a needle hydrophone setup as shown in Figure 3.3. For the acoustic tests a plexiglass sheet having the same properties as the wall of the machined slot (Figure 3.2b) was attached to the ultrasound sensor measurement surface with an oil-based couplant. The coupled sensor setup was placed in a glass characterization tank with deionized water at ~19 °C. The ultrasound beam from the ultrasound sensor was measured by the needle hydrophone, after propagating through the plexiglass sheet. A rectangular scanning grid (1 mm spatial resolution) across the sensors mid-plane was covered by moving the hydrophone with the linear axis. The scanning method used is described in detail by Shamu et al., (2016). The output from the acoustic characterization test is an acoustic color map from which the beam angle is determined. For the current study the Doppler angle was ~70.23°.

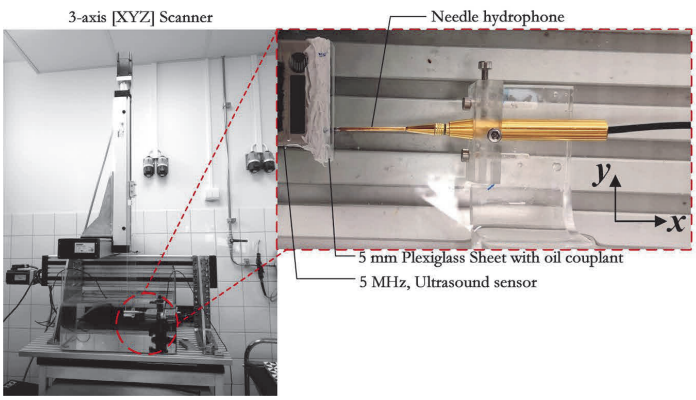

Figure 3.3: Acoustic characterization test setup showing the 3-axis scanner and the needle hydrophone test setup

The sound velocity was measured using a small stainless-steel cell setup (diameter of ~31 mm). A Carbopol sample at ~19 °C was placed in the cell and then 12 pulses were transmitted

into the sample. By using the Time of Flight (TOF) method, the traversing time was calculated and consequently the sound speed in Carbopol 0.1%wt; an average of ~1500 m/s.

UVP system: Once the correct Doppler angle and velocity of sound were determined, they were then used as input parameters to the UVP software of the Incipientus Flow Visualizer (IFV) system that was used for velocimetry within this study. The IFV has been developed over several years of extensive research for use in in-line rheological measurements of complex industrial fluids (Wiklund et al., 2007; Birkhofer, 2011; Berta et al., 2016; Rahman et al., 2017). The latest developments with the system have been on the ultrasound electronics and non-invasive sensors capable of measuring through industrial steel pipes (Shamu et al., 2016; Ricci et al., 2017; Rahman et al., 2017).

3.1.3 Carbopol gels: preparation and rheology

Carbopol gels prepared from Carbopol 980 (Lubrizol®, Belgium) were used in this study. The Carbomer powder (crosslinked polymer of acrylic acid) is supplied as a white powder which is then dispersed in distilled water, with the appropriate weighting to achieve the desired rheological properties. For the current study Carbopol powder was dispersed at 0.1% wt. of distilled water using a Silverson AX5 high shear mixer at ~1000 rpm for ~25 minutes (mixer shown in Figure 3.4). The dispersion was left to rest to expel air bubbles and allow complete hydration, before adding reflector particles needed for velocimetry, and a blue colorant. The final step in the preparation procedure was neutralizing the dispersion with dilute sodium hydroxide (18% wt. NaOH) to a final pH of ~6.5-7.5. The neutralization was done with a lower rpm mixer (135 rpm max.), since previous experimenters have shown that high shear mixing during the neutralization phase leads to polydisperse gels that exhibit significant rheological hysteresis (Dinkgreve et al., 2017; Dinkgreve et al., 2018; Di Giuseppe et al., 2015).

After the preparation and also after radial flow measurements in the flow loop the rheology of the Carbopol was measured using a vane (15 mm diameter, 38 mm height) in cup (30 mm diameter) geometry, and at 20 °C. The flow sweep was from 0.001 to 80 1/s with 10 points per decade in CSR mode allowing ~30 s per measurement point. Figure 3.5 shows the flow curve measurement. The measurement shows that the Carbopol exhibits simple YSF behavior that is well described by the HB model, with little to no observable rheological hysteresis in the flow curve.

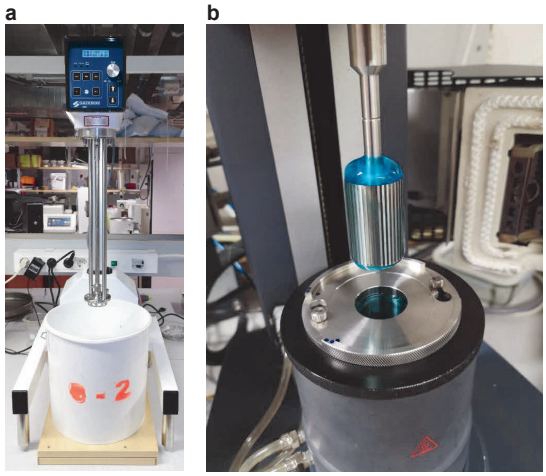

Figure 3.4. (a) High shear mixer (Silverson AX5) for dispersing Carbopol in distilled water (b) Image of a Carbopol gel with additional colorant and acoustic reflector particles.

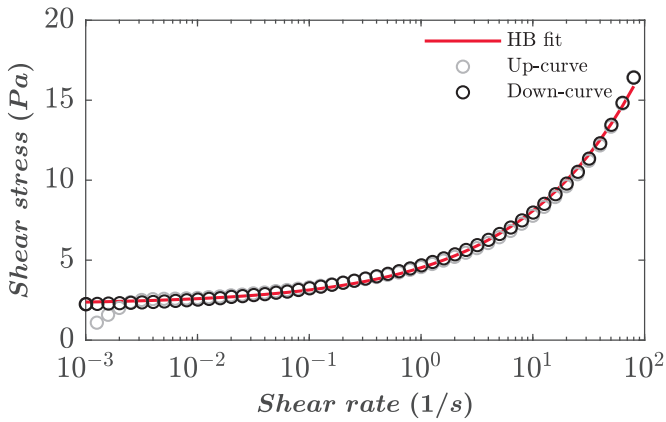

Figure 3.5. Flow curve measurement of Carbopol-980 gel at 0.1% w/w. Herschel Bulkley parameters determined as: $\boldsymbol{\tau_0}$ = 2.24 Pa, $\boldsymbol{k}$ = 2.28 Pa.s^n and $\boldsymbol{n}$ = 0.4.

3.1.4 Radial tests measurement procedure

The test procedure for acquiring radial flow velocity profiles ensures that the fluid measured is homogenous by first circulating the Carbopol fluid in the flow loop (Figure 3.3) for about 2 minutes at a high flow rate of ~58 l/min (similar to pre-shearing in a rheometer). Velocity profile measurements were then carried out by moving the ultrasound sensor to 17 different radial locations i.e. within the slot at radial lengths of 116 mm to 416 mm from the disk' center.

The factors that were varied were: three volumetric flow rates (Q1 = ~28 l/min, Q1 = ~40 l/min Q1 = ~58 l/min) and 3 apertures (5, 10, 15 mm). The fluid temperatures were recorded as ~18.5-20°C. Volume flow rate comparisons between the magnetic flow meter readings and the flow rates determined from the measured velocity profiles were carried out for all

measurement conditions. Reasonable agreement was achieved between the two methods of flow rate measurement. However, the major differences were in measurements within the 5 mm aperture. This discrepancy is most probably due to slight increases in the disk aperture due to higher pressure buildup when a small aperture is used. In general the wall position in velocimetry measurements is not well defined for smaller apertures due to the sample volume overlapping the fluid-plexiglass wall interface, which also could have contributed to the uncertainty (Wiklund et al., 2007). This wall issue can however be improved by reducing the number of cycles in an ultrasound pulse and increasing the ultrasound sensor central frequency. Some of the main ultrasound measuring parameters are listed here:

Table 1. UVP Measurement parameters during radial flow tests

Measurement parameter	**Value**
Ultrasound sensor frequency, f_0	5 MHz
Number of cycles per pulse	2
Number of pulse repetitions per pulse	256
Number of velocity profiles averaged	255
Gain setting (received signal)	26 dB
Transmission voltage (TX)	~80 Vpp
Velocity profile spatial resolution (with decimation), Δz	0.028 mm
Velocity of sound in Carbopol 0.1% wt.	~1490-1510 m/s
Velocity estimation method	Fast Fourier Transform (FFT)

Plug region detection: A custom algorithm to detect the plug-flow region in a velocity profile was also developed as part of the radial flow analysis.

The algorithm was based on the CUSUM calculation described by (Grigg et al., 2003), and was implemented with the Matlab® environment. The algorithm is as follows:

(i) The velocity profile is normalized ($V_z/V_z max$) and aperture distance (z/B)); and to this normalized profile fit a smoothing spline that minimizes the local fluctuations within the plug region of the profile. These fluctuations when significant, give rise to 'false' plugs due to local minima.

(ii) The standard deviation σ_V from 60% of the velocity points located in the region $[0 \leq z \leq 0.6(B)]$, is calculated as an approximation to the expected fluctuations within the plug region. The value of 0.6 is also an estimate based on the extent of the observable plug region across the aperture. A target median value $\tilde{x}_V$, is then calculated from 25% of the velocity points i.e. $[0 \leq z \leq 0.25(B)]$, these values are at the central core of the velocity profile and hence give a good approximate of the central plug velocity magnitude.

(iii) Using the CUSUM function from Matlab, with inputs from (i) and (ii), the plug position is then determined at the point z_p at which the velocity profile is 6 standard deviations ($6\sigma_V$) less than the target value ($\tilde{x}_V$).

4. RESULTS

Within this chapter the main findings from the velocity profiles measured in the radial flow model are discussed. The focus is on the plug-flow region and wall slip effects that in turn affected the overall shape of this region.

4.1 Radial flow model results

The velocity profiles measured within the radial flow model are presented in this section. The complete set of velocity profiles consists of 51 profiles per aperture, i.e. 17 different locations, at 3 flow rates per each of the 3 apertures. The velocity profiles are presented for the half-aperture, under the assumption that the velocity profile is axis-symmetric across half the aperture. Also, multiple reflections that are common in velocity profiles determined from UVP measurements distort the far wall data (i.e. opposite to the transducer wall).

4.1.1 Plug flow region and slip effects

An analysis of the velocity profiles carried out by normalizing the velocity profiles, i.e. scaling each velocity profile by its maximum central plug velocity $V_z max$ and the half aperture distance by the half of the aperture length B, gives $V_z/V_z max$ and z_p/B respectively. By plotting contour colormaps (Figure 4.1a,b,c) of the velocity profiles measured over the entire radial length, the rapid decrease in velocity magnitude, plus the distinct plug flow region are visualized. Also, the normalized profiles when overlaid in Figure 4.1d,e,f, show the relative extent of the plug region based on the CUSUM calculation, and the ratio of the slip velocity at the wall compared to the central plug velocity. Here, the contour plots and normalized velocity profiles are presented only for 1 flow rates and 3 apertures.

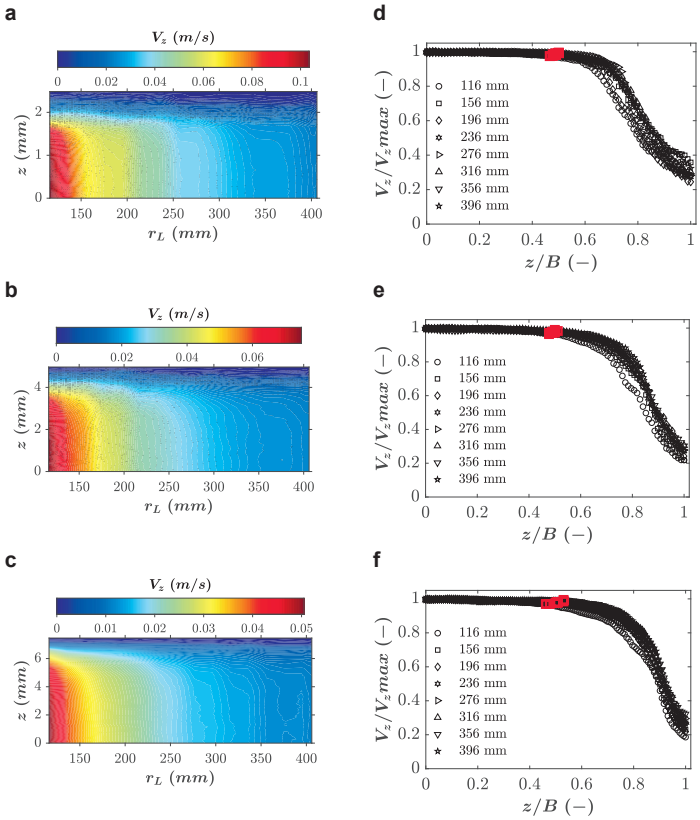

Figure 4.1. Contour colormaps of the velocity profiles at ~40 l/min, for apertures (a) 5 mm (b) 10 mm (b) 15 mm; the corresponding normalized velocity profiles (d) 5 mm (e) 10 mm (f) 15 mm. The red squares are plug region positions based on the CUSUM calculation.

As expected, significant wall slip effects were observed by the presence of finite wall velocities in all the measured velocity profiles. The slip velocity as a ratio of the maximum velocity per velocity profile (V_s/V_zmax) ranged between ~0.2-0.4 (Figure 4.1). Moreover, possibly due to slip, the CUSUM based plug ratios (z_p/B), were much larger ranging from ~0.45 to 0.55, compared to a maximum plug ratio of z_p/B = 0.21 predicted for the 15 mm aperture at the lowest flow rate.

4.1.2 Velocity profile comparisons with analytical solution

In Figure 4.2, the analytically predicted velocity profiles are compared to the measured velocity profiles. For all flow conditions, the magnitudes of the velocity profiles were within the same order of magnitude, and a good agreement was seen for profiles measured in the 5 mm aperture. However, it has to be pointed out that the 5 mm gap there could have been slight aperture increase due to much higher internal pressures, and hence the lowered velocity magnitude. However, this issue needs further investigation as part of the next study. Moreover, in general the analytical solution understated the velocities for the larger apertures 10 mm and 15 mm. It might be the case that the larger entrance effects expected in the 10 mm and 15 mm apertures dominate for most of the radial length. In line with this, the

agreement between the measured and predicted profiles is improved at the furthest radial location (396 mm) and at the lowest flow rate ~28 l/min. Lastly, the existence of secondary flows for a YSF like Carbopol is highly probable. Earlier radial flow experiments by Laurencena & Williams (1974) with tracer particles strongly suggested the presence of secondary flow, due to Carbopol gels' elasticity. Nevertheless, these and other related flow effects that could have been present in the radial flow data presented here need to be systematically studied and are out of the scope of the current work.

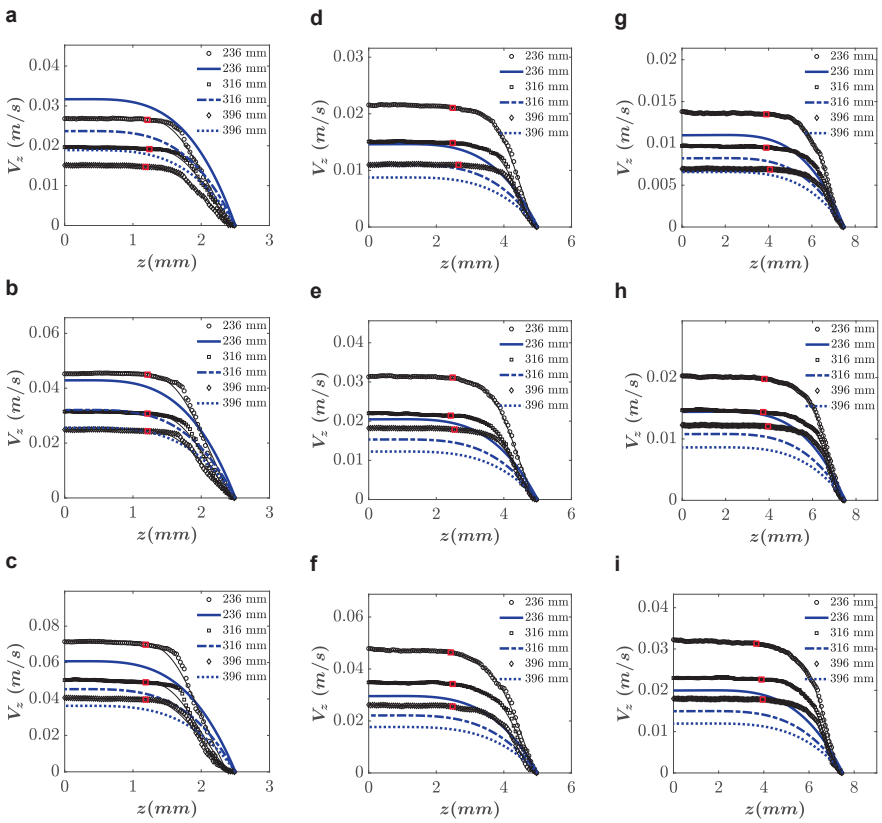

Figure 4.2. Analytically predicted profiles (thick blue lines) plotted together with the measured data (circles), for 5 mm aperture (a) ~28 l/min (b) ~40 l/min (c) ~58 l/min; 10 mm aperture (d) ~28 l/min (e) ~40 l/min (f) ~58 l/min; 15 mm aperture (h) ~28 l/min (i) ~40 l/min (j) ~58 l/min. The thin lines following the measured profiles are the smoothing splines used to estimate plug positions (red squares).

5. DISCUSSION, CONCLUSIONS AND SUGGESTIONS FOR FUTURE WORK

5.1 Radial flow of YSF between parallel disks

5.1.1 Discussion

2D-radial flow is an important flow configuration, and in grouting it is idealized as an approximation to radial grout spread in planar fractures. Analytical solutions have been presented for the radial flow configuration, however a few works have presented experimental studies to investigate the nature of radial flow velocity profiles, with focus on the plug-flow region that is associated to the yield stress of the fluid (Laurencena & Williams, 1974; Dai & Byron Bird, 1981; Lipscomb & Denn, 1984; Majidi et al., 2010; Mohammed, 2015; El Tani & Stille, 2017; Guo et al., 2017; Funehag & Thörn, 2018).

The study on radial flow presented in this work described the overall design of the radial flow model that was manufactured for measuring 2D radial flow velocity profiles, whilst using Carbopol a simple YSF, as the model fluid. In addition, the ultrasound sensor used for the radial flow experiment was also characterized to improve the accuracy of the measurements. Three apertures and three volumetric flow rates were used. A motorized linear axis was then moved to different radial locations to measure velocity profiles at constant flow conditions (flow rate, aperture).

An analysis of the measured velocity profiles showed that there was significant wall slip, which was expected due to the smooth walled plexiglass disks. The mechanism of slip which was assumed to be prevalent in the Carbopol radial flows, is that in which a thin micron-sized water-based film in the vicinity of the wall surrounds the bulk homogenous YSF. The consequence of the wall slip phenomena is less shear deformation within the bulk of the fluid, and hence the larger 'much flatter' measured plug-flow regions compared to the theoretical ones. The positions of the plug were calculated by using a CUSUM based algorithm that was developed as part of the current study. The plug detection algorithm proved to be effective since similar profiles were correctly assessed as having the same plug values.

When the measured profiles were compared to the analytical solution (Section 2.1), there was relatively good agreement at low flow rates and at the furthest points from the central inlet e.g. at 396 mm, and ~28 l/min. The agreement of the velocity profile magnitudes for the 5 mm apertures was greater; however, it must be noted that there was probably an aperture increase due to higher pressure build-up for the smallest aperture (5 mm). Additionally, the uncertainty in the wall position was higher for the 5 mm velocity profile measurements due to the sample volume overlapping with the wall interface.

5.2 Conclusions

In summary, the entire work was aimed understanding fundamental grout flow in planar fractures whilst visualizing radial flow velocity profiles in an experimental model. The main conclusions from this work, are summarized as follows:

- An experimental radial flow model was successfully designed and manufactured for the purpose of measuring, radial velocity profiles of a simple YSF model (Carbopol) flowing between smooth parallel disks.

- The experimental model system components were tested, and the ultrasound sensors were acoustically characterized to improve the accuracy of the measurements.
- Time averaged velocity profiles were successfully measured at three different apertures, three different flow rates and radial locations, showing the presence of a distinct plug flow region in all cases.
- As expected, significant wall slip effects were observed by the presence of a finite wall velocity in all profiles, which ranged from ~0.2-0.4 of the maximum profile velocity $V_z max$. After correction of the slip velocity V_s, the measured velocity profiles were lower, but reasonably within the same order of magnitude when compared to the analytically predicted ones. The major discrepancies were explained by the larger entrance effects in the larger geometries, probable aperture increase in 5 mm gap due to pressure buildup and also the likely presence of secondary flow effects that have been reported in previous studies.
- A CUSUM based algorithm was developed for this work to identify the extent of the plug flow region. The algorithm was efficient and robust enough to identify similar plug regions for similar profiles.
- The calculated plug region from the measured velocity profiles were larger than those predicted by the analytical solutions, possibly due to wall slip that reduces the deformation in the shear region of the profile.

On the whole, the studies showed that the rheological properties of YSFs can be measured with a higher degree of accuracy by considering the geometrical contributions (wall condition) and other mechanisms such as wall slip, thixotropy, flow localization, secondary flow and sedimentation complicate that tend to complicate the overall flow dynamics. Some of these flow phenomena e.g. secondary flow were not considered in detail as they were out of the scope of the current work. However, to better describe cement grout spread in rock fractures such complex mechanisms need to be considered as part of future studies.

5.2.1 Suggestions for future work

As part of the conclusions of the current work, some suggestions for future work are also summarized:

- For future work, the aim is to further study the nature of the plug-flow region, which remains an interesting fundamental question and especially for grouting design, where the radial flow configuration is often used. To carry out this detailed work, the current setup of the radial flow model could be improved by using higher frequency ultrasound sensors and different pulsar settings for enhanced lateral and axial resolution.

- The CUSUM method for plug detection that was developed as part of the current work, can still be improved, especially its robustness through testing different fluids and by varying the ultrasound measurement settings. In addition, the radial model spoke frame can be further reinforced with radial beams to prevent possible disk uplifts during high pressure flow conditions.

6. REFERENCES

Barber, W.D., Eberhard, J.W. & Karr, S.G. 1985. A new time domain technique for velocity measurements using Doppler ultrasound. *Biomedical Engineering, IEEE Transactions on*, (3): 213–229.

Berta, M., Wiklund, J., Kotze, R. & Stading, M. 2016. Correlation between in-line measurements of tomato ketchup shear viscosity and extensional viscosity. *Journal of Food Engineering*, 173: 8–14.

Birkhofer, B. 2011. Doppler Ultrasound-Based Rheology. In I. T. Norton, F. Spyropoulos, & P. Cox, eds. *Practical food rheology: an interpretive approach*. Food science and technology. Chichester, West Sussex ; Ames, Iowa: Wiley-Blackwell.

Birkhofer, B.H. 2007. *Ultrasonic In-Line Characterization of Suspensions*. Zurich, Switzerland: Laboratory of Food Process Engineering Institute of Food Science and Nutrition Swiss Federal Institute of Technology (ETH) Zurich ETH Zentrum, LFO 8092 Zurich Switzerland.

Chhabra, R. & Richardson, J. 2008. *Non-Newtonian Flow and Applied Rheology*. 2nd ed. Oxford, UK: Butterworth-Heinemann.

Dai, G. & Byron Bird, R. 1981. Radial flow of a Bingham fluid between two fixed circular disks. *Journal of Non-Newtonian Fluid Mechanics*, 8(3–4): 349–355.

Di Giuseppe, E., Corbi, F., Funiciello, F., Massmeyer, A., Santimano, T.N., Rosenau, M. & Davaille, A. 2015. Characterization of Carbopol® hydrogel rheology for experimental tectonics and geodynamics. *Tectonophysics*, 642: 29–45.

Dinkgreve, M., Denn, M.M. & Bonn, D. 2017. "Everything flows?": elastic effects on startup flows of yield-stress fluids. *Rheologica Acta*, 56(3): 189–194.

Dinkgreve, M., Fazilati, M., Denn, M.M. & Bonn, D. 2018. Carbopol: From a simple to a thixotropic yield stress fluid. *Journal of Rheology*, 62(3): 773–780.

Dogan, N., McCarthy, M.J. & Powell, R.L. 2005. Measurement of polymer melt rheology using ultrasonics-based in-line rheometry. *Measurement Science and Technology*, 16(8): 1684–1690.

El Tani, M. 2012. Grouting Rock Fractures with Cement Grout. *Rock Mechanics and Rock Engineering*, 45(4): 547–561.

El Tani, M. & Stille, H. 2017. Grout Spread and Injection Period of Silica Solution and Cement Mix in Rock Fractures. *Rock Mechanics and Rock Engineering*, 50(9): 2365–2380.

Fransson, Å., Funehag, J. & Thörn, J. 2016. Swedish grouting design: hydraulic testing and grout selection. *Proceedings of the Institution of Civil Engineers - Ground Improvement*, 169(4): 275–285.

Frigaard, I.A., Paso, K.G. & de Souza Mendes, P.R. 2017. Bingham's model in the oil and gas industry. *Rheologica Acta*, 56(3): 259–282.

Funehag, J. 2007. *Grouting of Fractured Rock with Silica Sol*. Göteborg, Sweden: Chalmers University of Technology.

Funehag, J. & Thörn, J. 2018. Radial penetration of cementitious grout – Laboratory verification of grout spread in a fracture model. *Tunnelling and Underground Space Technology*, 72: 228–232.

Grigg, O.A., Farewell, V.T. & Spiegelhalter, D.J. 2003. Use of risk-adjusted CUSUM and RSPRTcharts for monitoring in medical contexts. *Statistical Methods in Medical Research*, 12(2): 147–170.

Guo, J., Asce, M., Shan, H., Xie, Z., Li, C., Xu, H., Zhang, J. & Professor, A. 2017. Exact Solution to Navier-Stokes Equation for Developed Radial Flow between Parallel Disks. *J. Eng. Mech.*: 10.

Gustafson, G., Claesson, J. & Fransson, Å. 2013. Steering Parameters for Rock Grouting. *Journal of Applied Mathematics*, 2013.

Gustafson, G. & Stille, H. 2005. Stop criteria for cement grouting. *Felsbau*, 23(3): 62–68.

Håkansson, U. 1993. *Rheology of fresh cement-based grouts*. Stockholm: Royal Institute of Technology.

Hässler, L. 1991. *Grouting of Rock - Simulation and Classification*. PhD. Stockholm: Royal Institute of Technology (KTH).

Huang, D.C., Liu, B.C. & Jiang, T.Q. 1987. An analytical solution of radial flow of a bingham fluid between two fixed circular disks. *Journal of Non-Newtonian Fluid Mechanics*, 26(1): 143–148.

Jensen, J.A. 1996. *Estimation Of Blood Velocities Using Ultrasound: A Signal Processing Approach*. Cambridge University Press.

Kotze, R., Wiklund, J. & Haldenwang, R. 2012. Optimization of the UVP+ PD rheometric method for flow behavior monitoring of industrial fluid suspensions. *Applied Rheology*, 22: 42760–1.

Laurencena, B.R. & Williams, M.C. 1974. Radial Flow of Non-Newtonian Fluids Between Parallel Plates. *Transactions of the Society of Rheology*, 18(3): 331–355.

Lipscomb, G.G. & Denn, M.M. 1984. Flow of bingham fluids in complex geometries. *Journal of Non-Newtonian Fluid Mechanics*, 14: 337–346.

Majidi, R., Miska, S.Z., Ahmed, R., Yu, M. & Thompson, L.G. 2010. Radial flow of yield-power-law fluids: Numerical analysis, experimental study and the application for drilling fluid losses in fractured formations. *Journal of Petroleum Science and Engineering*, 70(3–4): 334–343.

McCarthy, K.L., Kerr, W.L., Kauten, R.J. & Walton, J.H. 1997. Velocity Profiles Of Fluid/Particulate Mixtures In Pipe Flow Using MRI. *Journal of Food Process Engineering*, 20(2): 165–177.

Mohammed, M.H. 2015. Study of cement-grout penetration into fractures under static and oscillatory conditions. *Tunnelling and Underground Space Technology*: 11.

Nejad Ghafar, A. 2017. *An Experimental Study to Measure Grout Penetrability, Improve the Grout Spread, and Evaluate the Real Time Grouting Control Theory*. Stockholm: KTH Royal Institute of Technology.

Pfund, D.M., Greenwood, M.S., Bamberger, J.A. & Pappas, R.A. 2006. Inline ultrasonic rheometry by pulsed Doppler. *Ultrasonics*, 44: e477–e482.

Powell, R.L. 2008. Experimental techniques for multiphase flows. *Physics of Fluids*, 20(4): 040605.

Rahman, M., Wiklund, J., Kotzé, R. & Håkansson, U. 2017. Yield stress of cement grouts. *Tunnelling and Underground Space Technology*, 61: 50–60.

Ricci, S. & Meacci, V. 2018. Data-Adaptive Coherent Demodulator for High Dynamics Pulse-Wave Ultrasound Applications. *Electronics*, 7(12): 434.

Ricci, S., Meacci, V., Birkhofer, B. & Wiklund, J. 2017. FPGA-Based System for In-Line Measurement of Velocity Profiles of Fluids in Industrial Pipe Flow. *IEEE Transactions on Industrial Electronics*, 64(5): 3997–4005.

Satomura, S. 1957. Ultrasonic Doppler Method for the Inspection of Cardiac Functions. *The Journal of the Acoustical Society of America*, 29(11): 1181–1185.

Savage, S.B. 1964. Laminar Radial Flow Between Parallel Plates. *Journal of Applied Mechanics*, 31(4): 594.

Shamu, T.J., Kotze, R. & Wiklund, J. 2016. Characterization of Acoustic Beam Propagation Through High-Grade Stainless Steel Pipes for Improved Pulsed Ultrasound Velocimetry Measurements in Complex Industrial Fluids. *IEEE Sensors Journal*, 16(14): 5636–5647.

Stille, H. 2001. Grouting-Research Work and Practical Application. In *4th Nordic Rock Grouting Symposium*. Stockholm.

Stille, H. 2015. *Rock grouting - Theories and Applications*. Stockholm: Vulkanmedia.

Takeda, Y. 1991. Development of an ultrasound velocity profile monitor. *Nuclear Engineering and Design*, 126: 277–284.

Takeda, Y. 2012. *Ultrasonic Doppler velocity profiler for fluid flow*. Tokyo, Japan: Springer.

Wiklund, J., Shahram, I. & Stading, M. 2007. Methodology for in-line rheology by ultrasound Doppler velocity profiling and pressure difference techniques. *Chemical Engineering Science*, 62(16): 4277–4293.

Zou, L., Håkansson, U. & Cvetkovic, V. 2019. Cement grout propagation in two-dimensional fracture networks: Impact of structure and hydraulic variability. *International Journal of Rock Mechanics and Mining Sciences*, 115: 1–10.

Zou, L., Håkansson, U. & Cvetkovic, V. Radial propagation of yield-power-law fluids into water-saturated homogeneous fractures.

Zou, L., Håkansson, U. & Cvetkovic, V. 2018. Two-phase cement grout propagation in homogeneous water-saturated rock fractures. *International Journal of Rock Mechanics and Mining Sciences*, 106: 243–249.

UTÖKAD SVENSK SAMMANFATTNING

1. INTRODUKTION

Injektering med cementbaserade injekteringsmedel utgör en viktig del inom anläggningsbyggandet i Sverige, tex vid tunneldrivning och dammbyggnad. Cementbaserade medel används främst pga dess relativt låga kostnad och dess skonsammare miljöpåverkan jämfört med kemiska injekteringsmedel. Miljödomar som föreskriver begränsad vatteninträngning i underjordiska tunnlar för att mildra konsekvenser för miljön, t.ex. sättningar och dränering av vattenresurser utgör krav för byggverksamheten [5]. Dessa krav, i kombination med behovet av att minska injekteringstiden och kostnaderna har lett till fokuserad injekteringsforskning som syftar till att förbättra cementbrukens strömningsegenskaper och deras karakterisering för praktisk användning.

Det nuvarande forskningsläget relaterat till cementbaserade injekteringsmedels strömningsegenskaper har nu nått en avancerad nivå, där ny digital teknik för kvalitetssäkring, t.ex. ultraljudsbaserade reologiska mätningar testas nu och optimeras för förbättring av injekteringsutförandet [6], [7].

Det ultimata målet är att kunna mäta de reologiska egenskaperna direkt och kontinuerligt under injekteringsprocessen in-line(figur 1c) för processtyrning och kvalitetskontroll, och därmed minska behovet av off-line-metoder och användning av opålitliga och simpla anordningar, t.ex. Marshkon i faktiska fältapplikationer (figur 1a). Enkla anordningar, såsom Marshkon, erbjuder endast en skenbar viskositet i motsats till hela flödeskurvan (se figur 1b). Det finns fortfarande mycket arbete som bör utföras för att förstå de underliggande fenomenen för den komplexa strömningen av cementbruk. Genom att skapa en ökad förståelse för dessa fenomen kan man möjliggöra en implementering av in-line metoder och en förbättring av injekteringsdesign och utförande.

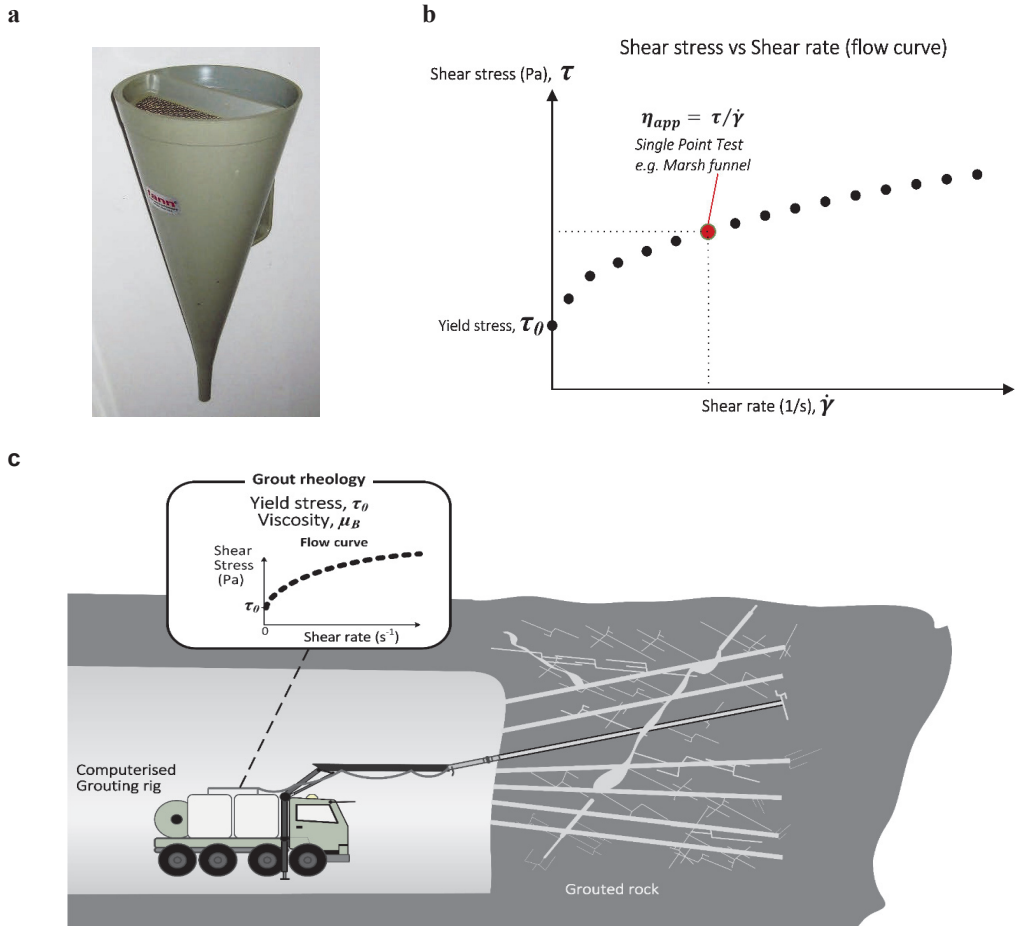

Figur 1. (a) Marshkon, (b) schematisk flödeskurva, (c) illustration av in-line mätning av reologin på cementbruk under pågående injektering.

För att studera nuvarande beräkningsmodeller inom injektering, som baseras på radiell strömning mellan två planparallella skivor, har en fysisk laboratoriemodell tagits fram. Flödet, hastighetsprofilen och pluggbildning jämförs mellan modellen och de teorier som idag används inom RTGC (Real Time Grouting Concept). Denna konfiguration, i vilken en vätska tränger in i mitten av två skivor är av intresse för injekteringsdesign, eftersom det idealiskt simulerar cementinjektering från ett centralt injektionsborrhål, varifrån bruket sprider sig radiellt utåt i omgivande sprickor [4], [9] (figur 2). Plugflödesregionen i hastighetsprofilen för en ”Yield-stress fluid” (YSF) är direkt relaterad till vätskans strömningsegenskaper (konstitutiva samband mellan skjuvspänning och deformationshastighet), eftersom pluggregionen är ett icke-skjuvat område, där spänningarna utmed spricköppningen är mindre än flytgränsen. Endast en begränsad mängd forskning har presenterat analytiska och numeriska lösningar som beskriver de förväntade

hastighetsprofilerna för (YSF) i denna flödesgeometri [5], [10], [11]. En experimentell studie som ett första steg mot verifiering av befintlig teori, baserad på mätningen av formen på pluggflödesregionen utmed den radiella inträngningen utgjorde också en viktig del av det nuvarande forskningsarbetet.

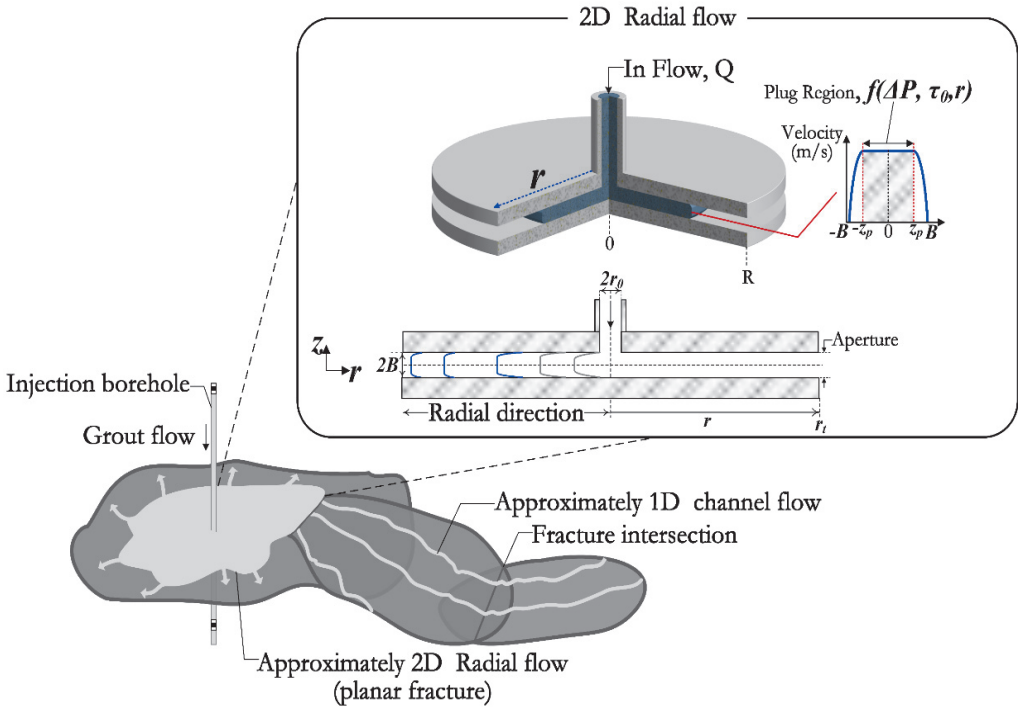

Figur 2. Schematisk illustrering av den idealiserade 2D-radiella flödeskonfigurationen och 1D-kanaler

1.1 Radiella Strömnings tester med Ultrasound Velocity Profiling (UVP)

Den ursprungliga utformningen av den fysiska radiella modellen baserades på modeller presenterade i litteraturen [12], [13]. Målet var att ha ett radiellt flöde som var fritt från hindrande föremål, t.ex. Fästelement, för att noggrant studera det radiella flödet av Carbopol. Hela uppställningen inklusive en bild av den faktiska modellen som används visas i figur 3. Komponenterna inkluderade en magnetisk flödesmätare (Discomag DMI 6531, Endress + Hausser) vid pumputtaget och en PT100-temperaturgivare.

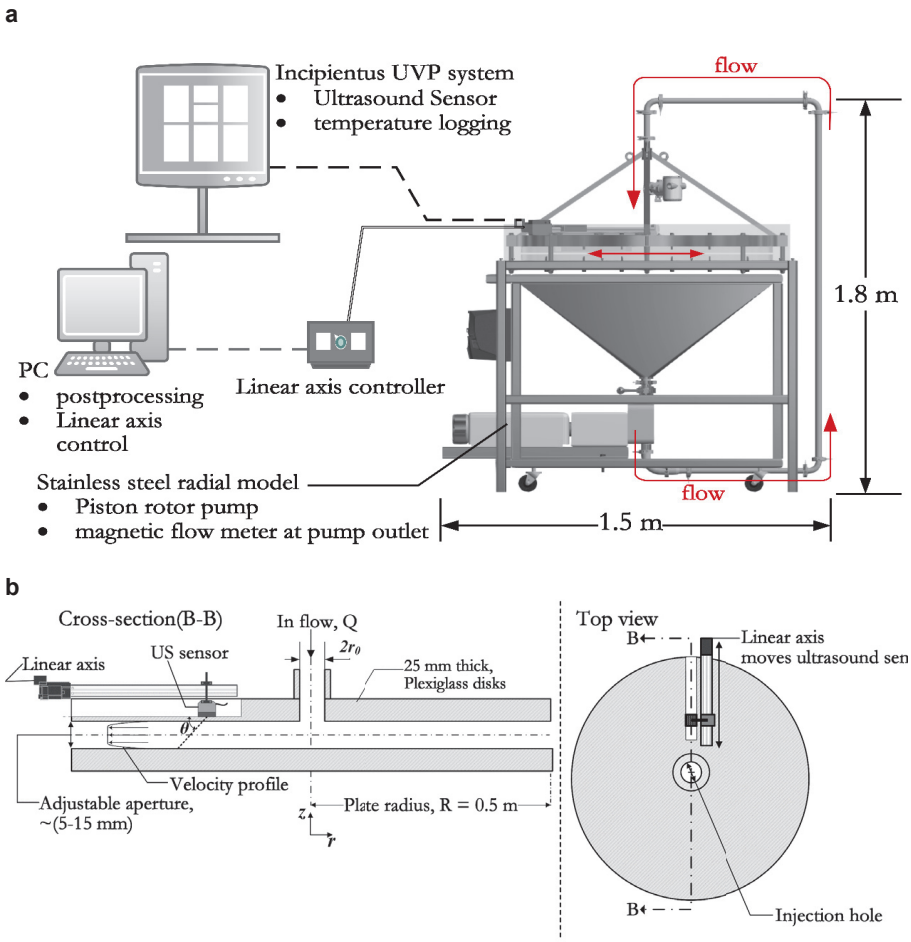

Figur 3. Radiell flödesmodell (a) schematisk illustration av det radiella flödessystemet (b) flödesområdet mellan de parallella plattorna och den motoriserade linjära axeln (c) bild som visar ultraljudssensor i slitsen (d) bild av ekerramen.

En kolvrotorpump används för att pumpa vätskan vid valda flödeshastigheter som reglerades från en frekvensomriktare (VSD). Vätskan cirkulerades sedan från botten av tanken in i det radiella flödesområdet där mätningen utfördes. En motoriserad linjär axel (Isel LEZ 1) med en repeterbarhet på ± 0,2 mm användes för att flytta ultraljudssensorn (US-sensorn figur 3b) som används för att erhålla hastighetsprofilen vid olika radiella avstånd. Scheman och bilder av den linjära axeluppsättningen och den radiella modellen visas i figur 3. Slitsen som visas i figur 3b och 3c skars i den övre skivan för att möjliggöra tillräcklig spridning av ultraljudstrålen, utan betydande dämpning pga skivans tjocklek. Efter bearbetningen var väggtjockleken i slitsen 5 mm (ursprungligen 25 mm). Den önskade spalten (öppningen) mellan skivorna uppnåddes med ett metalliskt distanssystem runt skivans periferi. Den övre ekramen användes som stöd för toppskivan för att bibehålla önskad öppning även vid höga flödes- och tryckförhållanden.

1.2 Carbopol

En modellvätska, Carbopol 980 (Lubrizol®, Belgien), användes för studien i stället för cement för att studera vätskans strömning utan störning från tixotropiska och tidsberoende (från hydratiseringen) effekter som är karakteristiska för cement. Carbopol vätskan framställdes enligt [14], [15] med blått färgämne och spårpartiklar för att underlätta ultraljudshastighetsmätningen. De reologiska parametrarna som var representativa för Carbopol var: Herschel Bulkley-parametrar τ_0 = 2,24 Pa, k = 2,28 Pasn och n = 0,4 (se [16]).

1.3 Mätning med ultraljud - Ultrasound Velocity Profiling (UVP)

UVP-metoden för att mäta hastighetsprofiler har använts för ett brett spektrum av komplexa vätskor, från livsmedelsprodukter till mineralsuspensioner [7], [17]. De individuella hastigheterna vid varje punkt i flödesgeometrin där hastighetsprofilen mäts beräknas som,

$$v_i = cf_{d_i}/2f_0 cos\theta$$

där f_0 är den centrala ultraljudstransmissionsfrekvensen, c är ljudets hastighet, f_{d_i} Doppler-växelfrekvensen för partiklar som strömmar vid ett visst avståndsläge (grind) och θ är Doppler-vinkeln. Flera studier har visat att noggrannheten för hastighetsuppskattningen beror på korrekt bestämning av ljudhastigheten i vätskan som studeras samt Doppler-vinkeln, där bidraget från felaktiga vinkelvärden är ganska betydande. Därför utfördes i detta arbete mätningen av denna vinkel i detalj med hjälp av en nålhydrofon enligt [18].

När rätt Doppler-vinkel och ljudets hastighet var bestämda användes de sedan som ingångsparametrar till UVP-mjukvaran för Incipientus Flow Visualizer (IFV) -systemet som användes i denna studie. Den senaste systemutvecklingen har skett beträffande elektronik och icke-invasiva sensorer, som kan mäta genom industriella stålrör [7], [18], [19] (www.incipientus.com). Hastighetsprofiler erhölls längs den radiella slitsen som visas i figur 3b. Före varje hastighetsprofil cirkulerades Carbopol vätskan först i flödesslingan under 2 minuter för att få en homogen vätska vid mätningen.

Pluggbestämning: Som en del av arbetet utvecklades en anpassad CUSUM plugg-algoritm för att uppskatta den relativa plugg-regionen i varje profil (se [16]). CUSUM-algoritmen syftade till att noggrant identifiera plugg-regionen i det strömmande tvärsnittet, genom en serie beräkningssteg. Först utjämnades originaldata för att minimera lokala fluktuationer och brus i hastighetsprofilen; denna profil normaliserades sedan i förhållande till den maximala hastigheten i tvärsnittet (dvs i mitten). Sedan beräknades medianvärdet samt standardavvikelsen för en fjärdedel av de totala hastighetspunkterna, som en tillförlitlig uppskattning av plugghastigheten. Slutligen beräknades startpositionen för plugg-regionen som den punkt vid vilken hastighetsprofilstorleken var 6 standardavvikelser under medianvärdet för plugghastigheterna.

2. RESULTAT

2.1 Hastighetsprofiler vid radiell strömning

Hastighetsprofilerna uppmätta i den radiella flödesmodellen visade att det för vätskor med en flytgräns spänning, existerar en distinkt plugg vid radiellt flöde. Som väntat för släta plexiglasväggar fanns det en betydande glidning vid väggarna som noterades som vägghastigheter skilt från noll, dvs. ~ 0,2-0,4 av den maximala axiella hastigheten (figur 4d, e, f). Efter korrigering för glidning, blir det en relativt bra överensstämmelse mellan de analytiska bestämda hastighetsprofilerna och de uppmätta (Figur 4b). Glidningen ökade troligen också den totala pluggtjockleken på grund av mindre skjuvdeformation. Dessutom kan pluggen form ha ökat betydligt genom sekundärt flöde på grund av Carbopol vätskans elasticitet. Dessa och andra relaterade flödeseffekter som kunde ha varit närvarande i de radiella data som presenteras här måste systematiskt studeras vidare men ligger utanför ramen för det aktuella arbetet i denna avhandling.

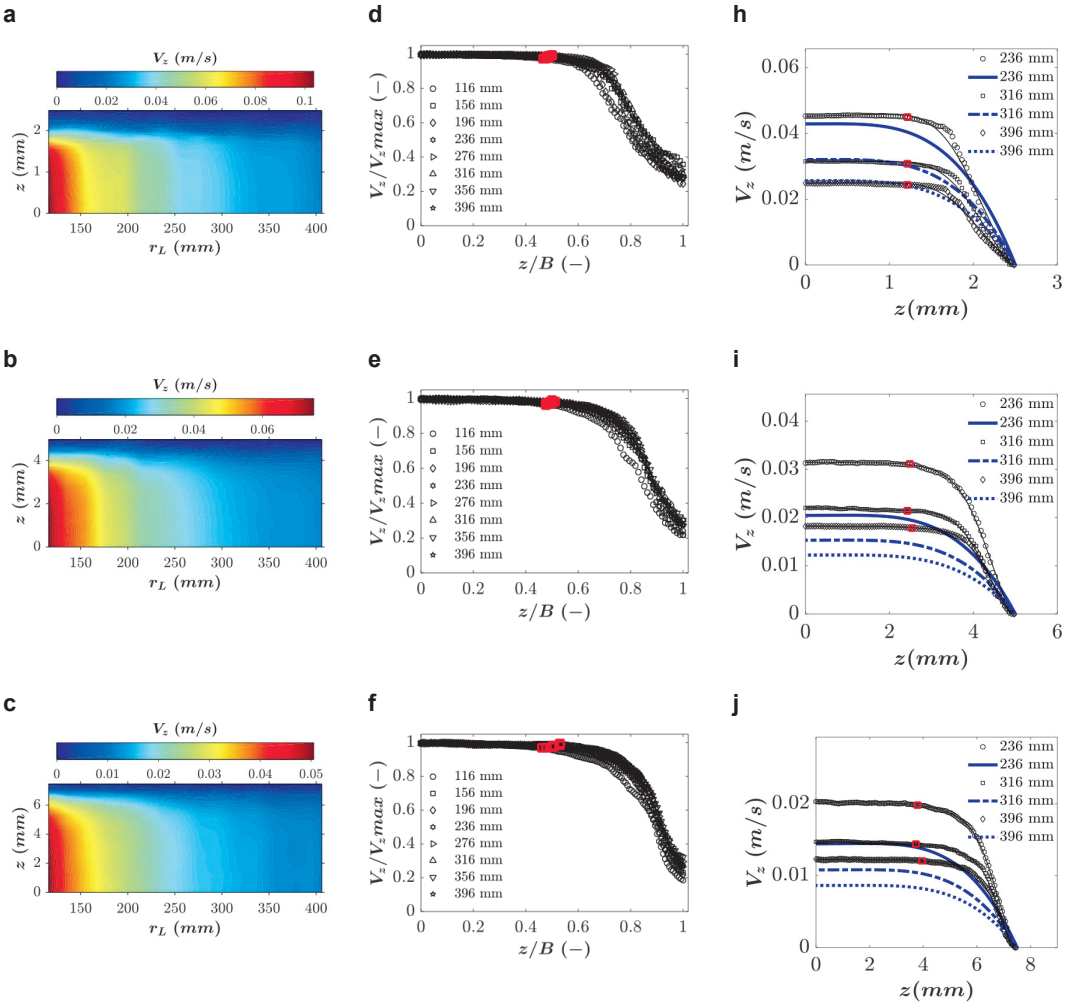

Figur 4. Färgkonturer för hastighetsprofilerna vid 40 l/min, för öppningar (a) 5 mm, (b) 10 mm och (c) 15 mm; motsvarande normaliserade hastighetsprofiler (d) 5 mm, (e) 10 mm och (f) 15 mm, de röda rutorna är pluggregionen baserat på CUSUM-beräkningen; jämförelser av analytiska och uppmätta hastighetsprofiler vid vald radiell position (h) 5 mm, (i) 10 mm och (j) 15 mm.

3. SLUTSATSER OCH FÖRSLAG PÅ FORTSATT ARBETE

Syftet med detta arbete har varit att bättre förstå reologiska mätningar gjorda på cementbruk och andra ”Yield-stress fluids” (YSF) och deras tillämpning vid injektering av bergsprickor. De viktigaste slutsatserna från detta arbete sammanfattas enligt följande:

- För radiell strömning användes ultraljudshastighetsmätningen framgångsrikt för att mäta radiella hastighetsprofiler. Mätningarna visade att det finns distinkta pluggregioner, och för längden på den använda experimentella modellen var pluggen relativt konstant. De aktuella resultaten är emellertid inte helt entydiga eftersom det fanns en viss skillnad jämfört med analytiska förutsägelser som behöver ytterligare undersökning.

- Dessa skillnader förklaras av närvaron av glidning vid väggarna, otillräckliga längder för att uppnå utbildad strömning, vissa felaktigheter i data nära väggarna och den troliga förekomsten av sekundära flöden.
- I framtiden kommer arbetet med mätning av cementbruk att fokuseras på att utveckla de befintliga in-line metoderna för kontinuerlig mätning baserat på ultraljud, samtidigt som man använder den kunskap som samlas in från de off-line mätningar som idag utförs. När det gäller den radiella modellen kommer några justeringar av den existerande modellen att utföras.

4. REFERENSER

[1] U. Håkansson, “Rheology of fresh cement-based grouts,” KTH Royal Institute of Technology, Stockholm, 1993.

[2] Å. Fransson, J. Funehag, and J. Thörn, “Swedish grouting design: hydraulic testing and grout selection,” *Proceedings of the Institution of Civil Engineers - Ground Improvement*, vol. 169, no. 4, pp. 275–285, Nov. 2016.

[3] L. Zou, U. Håkansson, and V. Cvetkovic, “Two-phase cement grout propagation in homogeneous water-saturated rock fractures,” *International Journal of Rock Mechanics and Mining Sciences*, vol. 106, pp. 243–249, Jun. 2018.

[4] H. Stille, *Rock grouting - Theories and Applications*. Stockholm: Vulkanmedia, 2015.

[5] G. Gustafson, J. Claesson, and Å. Fransson, “Steering Parameters for Rock Grouting,” *Journal of Applied Mathematics*, vol. 2013, 2013.

[6] M. Rahman, U. Håkansson, and J. Wiklund, “In-line rheological measurements of cement grouts: Effects of water/cement ratio and hydration,” *Tunnelling and Underground Space Technology*, vol. 45, pp. 34–42, Jan. 2015.

[7] M. Rahman, J. Wiklund, R. Kotzé, and U. Håkansson, “Yield stress of cement grouts,” *Tunnelling and Underground Space Technology*, vol. 61, pp. 50–60, Jan. 2017.

[8] T. J. Shamu and U. Håkansson, “Rheology of cement grouts: On the critical shear rate and no-slip regime in the Couette geometry,” *Cement and Concrete Research*, p. S0008884619301437, May 2019.

[9] U. Håkansson, “Rheology of fresh cement-based grouts,” Royal Institute of Technology, Stockholm, 1993.

[10] G. Dai and R. Byron Bird, “Radial flow of a Bingham fluid between two fixed circular disks,” *Journal of Non-Newtonian Fluid Mechanics*, vol. 8, no. 3–4, pp. 349–355, Jan. 1981.

[11] T. J. Shamu, L. Zou, R. Kotzé, J. Wiklund, and U. Håkansson, “Radial flow velocity profiles of a yield stress fluid between smooth parallel disks,” Apr-2019.

[12] S. B. Savage, “Laminar Radial Flow Between Parallel Plates,” *Journal of Applied Mechanics*, vol. 31, no. 4, p. 594, 1964.

[13] B. R. Laurencena and M. C. Williams, “Radial Flow of Non-Newtonian Fluids Between Parallel Plates,” *Transactions of the Society of Rheology*, vol. 18, no. 3, pp. 331–355, Sep. 1974.

[14] M. Dinkgreve, M. M. Denn, and D. Bonn, “‘Everything flows?’: elastic effects on startup flows of yield-stress fluids,” *Rheologica Acta*, vol. 56, no. 3, pp. 189–194, Mar. 2017.

[15] E. Di Giuseppe *et al.*, “Characterization of Carbopol® hydrogel rheology for experimental tectonics and geodynamics,” *Tectonophysics*, vol. 642, pp. 29–45, Feb. 2015.

[16] T. J. Shamu, “On the measurement and application of cement grout rheological properties,” KTH Royal Institute of Technology, Stockholm, 2019.

[17] J. Wiklund, I. Shahram, and M. Stading, “Methodology for in-line rheology by ultrasound Doppler velocity profiling and pressure difference techniques,” *Chemical Engineering Science*, vol. 62, no. 16, pp. 4277–4293, Aug. 2007.

[18] T. J. Shamu, R. Kotze, and J. Wiklund, “Characterization of Acoustic Beam Propagation Through High-Grade Stainless Steel Pipes for Improved Pulsed Ultrasound Velocimetry Measurements in Complex Industrial Fluids,” *IEEE Sensors Journal*, vol. 16, no. 14, pp. 5636–5647, Jul. 2016.

[19] S. Ricci, V. Meacci, B. Birkhofer, and J. Wiklund, “FPGA-Based System for In-Line Measurement of Velocity Profiles of Fluids in Industrial Pipe Flow,” *IEEE Transactions on Industrial Electronics*, vol. 64, no. 5, pp. 3997–4005, May 2017.

BeFo

Box 55545
SE-102 04 Stockholm

info@befoonline.org • www.befoonline.org
Visiting address: Sturegatan 11, Stockholm

ISSN 1104-1773